

ORIGINAL ARTICLE

Performance Comparison Between Predictive Functional Control and PID Algorithms for Automobile Cruise Control System

M.A.S. Zainuddin^{1,2}, M. Abdullah^{1,*}, S. Ahmad¹, and K.A. Tofrowaih³¹Department of Mechanical Engineering, International Islamic University Malaysia, Jalan Gombak, 53100, Kuala Lumpur, Malaysia²Department of Automotive Engineering Technology, Kolej Kemahiran Tinggi MARA, Masjid Tanah, 78300 Melaka, Malaysia³Department of Mechanical and Manufacturing Engineering, University Teknikal Malaysia Melaka, Hang Tuah Jaya, 76100 Melaka, Malaysia

ABSTRACT – This work presents a performance comparison between a Predictive Functional Control (PFC) and a traditional Proportional Integral Derivative (PID) controller specifically for a cruise control application. The tuning efficacy, constraints handling, and disturbance rejection features of both controllers are analysed by comparing their closed-loop response. A simplified nonlinear vehicle longitudinal dynamics model is derived and utilised as a plant to simulate the control response from a real car. For a fair comparison, both PFC and PID are tuned to achieve the similar desired closed-loop time response. Qualitatively, the results show that PFC provides a better closed-loop response, constraints handling, and disturbance rejection compared to PID. Besides, it is also found that the tuning approach of PFC is more intuitive and practical in nature which can be very handy for the future development of an autonomous cruise control application.

ARTICLE HISTORYReceived: 24th Aug 2021Revised: 14th Oct 2021Accepted: 14th Feb 2022**KEYWORDS***Cruise control;**Predictive control;**Model predictive control;**PID control;**Tuning performance*

INTRODUCTION

The cruise control system is the most basic form of an Advanced Driver Assistant System (ADAS), where its primary function is to automatically regulate or maintain a vehicle's speed at the desired preference with regards to road condition and environment. This system can be very beneficial, especially for long-distance travel in a steady high-speed driving condition. Since the throttle paddle is controlled automatically, the cruise control system may reduce both: the driver body fatigue and also fuel consumption [1]. There are several variations in cruise control technology, which depend on automation capability, ranging from maintaining a current speed, tracking a new desired speed, and complete braking control [2]. It is also noted that most of the recent research and development works are focusing on the performance optimization between fuel consumption, passenger comfort, and safe distancing [3-6].

One of the limitations of conventional cruise control systems is that they can only work in high-speed driving conditions (more than 40 km/hour). This is because the designing process of a controller for this operation is more straightforward since the vehicle dynamics is assumed to be in a steady-state condition [7]. Compared to the low-speed operation, the vehicle dynamics becomes more complicated due to the nonlinearity, varying gear ratio selection and other parameter uncertainties. Although a more advanced version of cruise control with a stop and go function has been introduced in the market to tackle this issue, it is found out that the system response can be very slow and not responsive depending on what types of control algorithm and structure that its use [8].

Considerable research attempts have been made on utilizing the Proportional-Integral-Derivative (PID) controller for the cruise control, as discussed by various authors [9,10]. The PID controller is a traditional control algorithm that is widely employed in various industrial applications. The key selling points are its cost-effectiveness together with the well established theoretical framework. Generally, the core idea is to select a suitable value for the proportional (K_p), integral (K_i), and derivative (K_d) gains to get the desired performance. Nevertheless, finding the optimum balance between those three values is not as straightforward as one think. Although several procedures such as Ziegler Nichols or auto-tune function can be used as a guideline, the tuning parameters are not intuitive, which may become a problem for a less experienced user [11]. Another limitation with the PID controller is when handling a system constraint, where for some cases, it may lead to over saturation and wind-up [12].

On the other hand, a predictive controller provides a more systematic approach. It uses a simplified mathematical model to predict future outcomes and optimize the control input using a quadratic cost function while respecting system constraints [13]. MPC has achieved considerable success in a variety of practical applications, including the automotive, chemicals, aerospace, and food processing industries, thanks to the massive development of control theory [14]. MPC has had a significant impact on the direction of industrial control systems and a scientific study due to its appealing properties. This controller is well known for its optimality and has been a famous area of research in cruise control system development. However, one of the main drawbacks of MPC is that it requires high computation intensity. Within a single sampling time, the controller needs to compute an optimal control by making a prediction and optimization process. This requirement may not be a problem for a slow dynamics process; however, for fast application, the computation is critical

where a high power and large memory processor is often needed, leading to a relatively expensive or impractical implementation [15].

Surprisingly, a Predictive Functional Control (PFC) which is the simplified version of MPC seems to receive a lack of attention in academic research due to its suboptimal performance and lack of theoretical guarantee and assurance. Nevertheless, PFC can become an attractive alternative to the traditional PID controller for a simple application such as cruise control due to its simplicity and intuitive tuning procedure. There are also a few works of literature that compare the control performance of PFC and traditional PID control where the results are generally pointing to PFC's superiority and mainly in the robotics and chemical application [16]. The direct use of desired settling time or closed-loop time response as the main tuning parameter makes the designing process more transparent [17]. Besides, PFC also inherits several advantages of MPC algorithms, such as the systematic handling of constraints and delays control problems [18]. Due to the simplification in the control law, PFC coding becomes straightforward and only requires minimal computation, and indeed for this single-input and single-output (SISO) application, the coding is almost trivial.

Hence, the main aim of this paper is to compare the closed-loop performance between PFC and PID, where the focus of the analysis will be on the tuning effect, constraints handling, and disturbance rejection for the cruise control application. It should be noted that PFC should not be compared with MPC as the level of complexity in the optimization process is very different [19]. The structure of this paper is organized as follows. Section 2 presents the methodology and formulation of the simplified nonlinear vehicle longitudinal dynamics model and the PFC control law. Section 3 provides the simulation result where the response of PID and PFC are compared and analyzed. Section 4 summarizes the findings with some concluding remarks and possible future works.

VEHICLE LONGITUDINAL DYNAMICS

This section provides a brief explanation for the standard vehicle longitudinal dynamics mathematical model [20] that will be used in this work. This model only covers the dynamics from vehicle traction force to velocity. The actuation from power train dynamics and braking system are assumed to be well controlled, and any development for these parts constitute future work.

Equation of Motion for Vehicle Dynamic

The vehicle longitudinal dynamic is derived based on Newton's second law, where Figure 1 shows the basic force distribution on a vehicle.

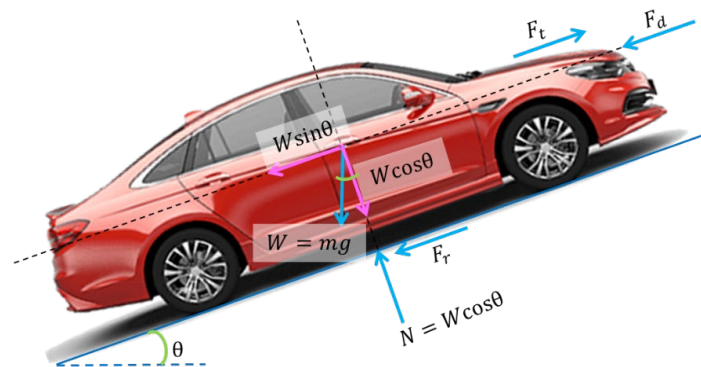


Figure 1. Forces distribution of vehicle climbing a hill.

The positive sense of horizontal direction is assumed to be in line with the vehicle motion, and the vertical direction is assumed to be in the perpendicular direction. The summation of the force can be represented via this equation:

$$F_t - mg \sin\theta - F_r - F_d = ma \tag{1}$$

where F_t is the total traction force from all the tires, F_r is the rolling resistance force, F_d is the aerodynamics force, g is the gravitational constant, θ is the inclination angle of the road, m is the mass of a vehicle, and a is the acceleration. The traction force F_t is assumed as the input to the system, while the rolling resistance force F_r and aerodynamics force can be represented as in Eq. (2) and Eq. (3), respectively [20].

$$F_r = fmg \cos\theta \tag{2}$$

$$F_r = F_d = 0.5\rho AC_d(v + v_w)^2 \tag{3}$$

The parameter f is the rolling resistance coefficient, ρ is the air density, A is the front area of the vehicle, C_d is the drag coefficient, v is the vehicle speed and v_w is the wind gust velocity. For simplicity, it should be noted the presented model is derived based on a lump parameter assumption. For a high-fidelity mathematical model, an interested reader can refer to these references [20,21].

Model Linearization

To implement a linear controller, the nonlinear mathematical model of Eq. (1) needs to be linearized with respect to its nominal operating points, where all the parameters need to be in the steady-state condition. Let acceleration a equals to \dot{v} and by using a Taylor series expansion, Eq. (1) can be linearized with respect to the nominal values of v_n , v_{wn} , θ_n , $F_{t,n}$ as:

$$m\dot{v}' = F_t' + mg(f\sin\theta_n - \cos\theta_n)\theta' - \rho AC_d(v_n + v_{wn})v' \quad (4)$$

The superscript $\{'\}$ in Eq. (4) denotes the difference between actual and nominal values [20]. With a simple algebraic manipulation, Eq. (4) can be further simplified into:

$$\tau\dot{v}' + v' = K(F_t' + d) \quad (5)$$

where

$$\tau = \frac{m}{\rho AC_d(v_n + v_{wn})}, \quad K = \frac{1}{AC_d(v_n + v_{wn})}, \quad d = mg(f\sin\theta_n - \cos\theta_n)\theta'$$

By using the Laplace transform, the linear transfer function of vehicle longitudinal dynamics can be represented as:

$$v'(s) = \frac{K}{\tau s + 1} [F_t'(s) + d(s)] \quad (6)$$

where the input to the system is the traction force F_t' , the output is velocity v' and the term d is assumed as a disturbance to the system.

Condition of Constraints and Disturbance

System constraint is one of the important information that can provide a logical sense when designing a controller. The controller needs to comply with the physical limitation of a system. In this example, only one input constraint was evaluated, with the maximum tractive force for both PID and PFC being limited to 2500N. In order to assess the robustness of the controller, two unmeasured disturbances are considered. First, an average of 200 kg mass is added to the vehicle weight to represent four additional passengers in the simulation. Secondly, at 300s, an inclination angle of 8.13 degree is introduced that mimic the Genting Highland – Batang Kali road (maximum slope of 14.2% gradient) [22].

Predictive Functional Control Formulation

Since Predictive Functional Control (PFC) is a discrete controller, the transfer function in Eq. (6) needs to be discretized with sampling time T_s . Let $y(z)$ denotes the output of the system and $u(z)$ as the control input. The discrete transfer function of Equation 6 can be represented as:

$$y(z) = \frac{b}{1 - az^{-1}} u(z) \quad (7)$$

where a and b are the discrete numerator and denominator, respectively. Generally, the framework of PFC can be divided into four components: the prediction structure, target trajectory, control law, and constraint handling.

Prediction Structure from Mathematical Model

The PFC concept mimics human intuition, where one would predict a future outcome and adjust the control action to reach the desired target. The one step ahead prediction structure, $y(k+1|k)$ at sample time k of Eq. (7) can be formed as:

$$y(k+1|k) = bu(k) + ay(k) \quad (8)$$

By utilizing a superimposed linear prediction structure [13] to Eq. (8), the n th step ahead prediction can be represented as:

$$y(k+n|k) = HU + Fy(k) \quad (9)$$

where,

$$H = \begin{bmatrix} b & 0 & 0 & 0 \\ ab & b & 0 & 0 \\ \vdots & \vdots & \ddots & \vdots \\ a^{n-1}b & a^{n-2}b & \dots & b \end{bmatrix}, U = \begin{bmatrix} u(k) \\ u(k+1) \\ \vdots \\ u(k+n) \end{bmatrix}, F = \begin{bmatrix} a \\ a^2 \\ \vdots \\ a^n \end{bmatrix}$$

Remark 1: The prediction structure for Eq. (8) is only valid for a first-order system. A higher-order system may need other information such as past inputs $u(k-1)$ and outputs $y(k-1)$, which depends on the size and nature of a system. A detailed derivation for a standard transfer function can be found in this reference [13].

Target Trajectory

The core principle of PFC is that at each sample time k , a new target trajectory is calculated based on a desired steady-state target R . Although the dynamics of the trajectory can take any form, the simplest one is by assuming a first-order response [20] from the measured output y_p to R . Hence, the n th step ahead trajectory can be defined as:

$$r(k+n|k) = (1 - \lambda^n)R + \lambda^n y_p(k) \tag{10}$$

It should be noted that there are two main tuning parameters for PFC. The first one is the desired closed-loop pole λ . For industrial users, this term is usually converted to the desired Closed-Loop Time Response (CLTR), which determines the convergence speed to reach 95% of a steady-state value [17]. The relationship is given as:

$$\lambda = e^{-3T_s/CLTR} \tag{11}$$

The second tuning parameter is the number of coincidence horizon n . This is a point where the model prediction from Eq. (9) is forced to match with the target trajectory, as shown in Figure 2.

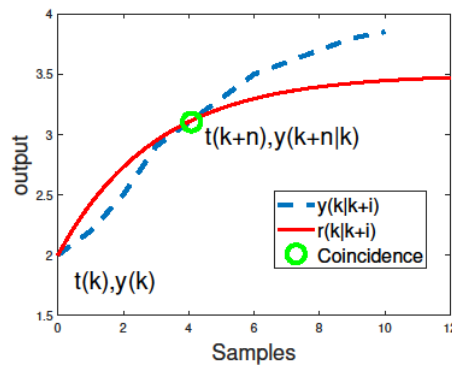


Figure 2. Model prediction and target trajectory of PFC at the first-time step.

Remark 2: The tuning procedure in the cruise control application is straightforward since the representative model is a first-order system. Hence, the usual practice is to set $n=1$ [23]. However, there is a trade-off in this selection such that if n is low, it will lead to an open-loop prediction mismatch or an ill-posed solution. There are some possible solutions as reported in [24, 25]. But this issue will not significantly impact this application as no output constraints were considered.

Control Law

As mentioned in the previous subsection, the fundamental law of PFC is to force the model prediction in Eq. (9) with the desired target trajectory in Eq. (10) at a selected coincidence horizon n . Nevertheless, the prediction mismatch between model and actual value should be considered in the control law and hence:

$$y(k+n|k) + d(k) = r(k+n|k) \tag{12}$$

The term $d(k) = y_p(k) - y(k)$ represents the difference between measured output and model output for handling parameter uncertainty, noise, and disturbance [17].

$$h_n u(k) + F_n y(k) + d(k) = (1 - \lambda^n)R + \lambda^n y_p(k) \tag{13}$$

With a simple algebraic manipulation, the control input of PFC is computed as:

$$u(k) = h_n^{-1} [(1 - \lambda^n)R + \lambda^n y_p(k) - F_n y(k) + d(k)] \tag{14}$$

Based on the receding horizon principle, the whole procedure is repeated at each time step.

Constraints Handling

One of the advantages of PFC is its ability to handle the process constraints, including input, rate, state, or output [24]. For the cruise control setup, only the input constraint is considered where it can be translated into the maximum traction force that a vehicle can produce. Without explicitly including this constraint in the control law, a simple clipping method can be used as if $u(k)$ is larger than u_{max} , then set:

$$u(k) = u_{max} \quad (15)$$

Nevertheless, it is important for the prediction model in Eq. (15) to detect a possible violation *a priori* [17] to avoid any possible overshoot in the output due to the mismatch between model and actual behaviour.

Remark 3: The clipping method is straightforward, yet it may negatively impact certain applications, especially if it is used with a PID controller. Several methods have been introduced in the literature to overcome this drawback, such as integral wind-up and smith predictor [26]. However, the main challenge for this method is to come out with a systematic tuning procedure as most of the problems is system dependent. Conversely, due to the prediction nature of PFC, the saturation problem is eliminated with the condition that the constraints are not very tight. It has been proved in many papers [24,27,28] that the constraints handling of PFC is recursive feasible since the future input dynamics is constant, where any change in the first sample input will not contradict with the following sample.

RESULTS AND ANALYSIS

This section presents the performance comparison between the proposed PFC controller and traditional PID controller based on the simplified nonlinear vehicle longitudinal dynamic model by using MATLAB®/Simulink® software. This nonlinear model has been derived in the earlier section and utilized as a plant to simulate the control response of a real car. The vehicle and surrounding parameters for the simulation are selected based on *Proton Perdana (second generation)* parameters as provided in Table 1 below [29]:

Table 1. Parameters for the longitudinal vehicle model.

Parameters	Value
Curb weight	1535 kg
Frontal Area	1.88 m ²
Wheel radius	0.317 m
Air density, ρ	1.202 kg/m ³
Drag coefficient, C_d	0.31
Gravity acceleration, g	9.81 m/s ²
Rolling resistance coefficient	0.015
Wind gust, v_{wn}	2 m/s

As discussed in the previous section, the nonlinear model needs to be linearized with respect to nominal operating points. All the parameters for the nominal operating points are set as shown in Table 2 below. In this case, the nominal traction force $F_{t,n}$ is calculated using the derived Eq. (4), which is 395.40 N by assuming the steady-state condition, $\frac{dv}{dt} = 0$.

Table 2. Parameters for the nominal operating points.

Parameters	Value
Nominal vehicle speed, v_n	20 m/s
Nominal wind gust speed, v_{wn}	2 m/s
Nominal slope angle, θ_n	0 degree
Nominal traction force, $F_{t,n}$	395.40 N

Once the continuous linear model is obtained as in Eq. (6), it is then discretized with 0.1 s sampling time (T_s). For each simulation case, two graphs will be presented where one corresponding to the system input (*vehicle's tractive force*) and another is for the system output (*vehicle's output velocity*). The closed-loop comparison between PFC and PID focused on four areas:

- i. Efficacy of tuning parameter for the closed-loop response.
- ii. Response of the closed-loop without any system constraints.
- iii. Response of the closed-loop with input tractive force constraints.
- iv. Response of the closed-loop in the presence of disturbances.

As for the generic design objective, the proposed controller should not produce significant overshoot, fast settling time, and minimal root mean square error, RMSE. Furthermore, the required input should not be overly aggressive, as this would affect the driver's comfort and the vehicle's fuel consumption. It also should be able to handle vehicle

constraints and external disturbances such as limitation of tractive force, the addition of passenger weight and inclination of road angle.

Enhancing Tuning Efficacy of PID and PFC

For this case, the PID and PFC controllers are tuned with respect to their own tuning rules for the cruise control application. Since the PID controller is not the main contribution of this paper, an auto-tune function in MATLAB is used to get the desired response. Two parameters need to be selected in the Transfer Function Based (PID Tuner App) tuning method, which are the expected response time and level of robustness. Based on these selections, the three PID gains were generated automatically.

By fixing a maximum level of robustness which is 0.9, Figure 3 shows the closed-loop response of PID controller with varying response time in tracking 20 m/s from rest for the first 120 s and 25 m/s (black dashed line) for the remaining simulation time. Although a significant impact can be observed from the closed-loop response, it is found that the selected desired response time does not reflect the actual closed-loop response behaviour. In most cases, the actual response time is longer than the desired one, although this can be changed if the robustness property is set to be more aggressive. Besides, there is a noticeable overshoot in the output response corresponding to a high over actuation input computed by the controller.

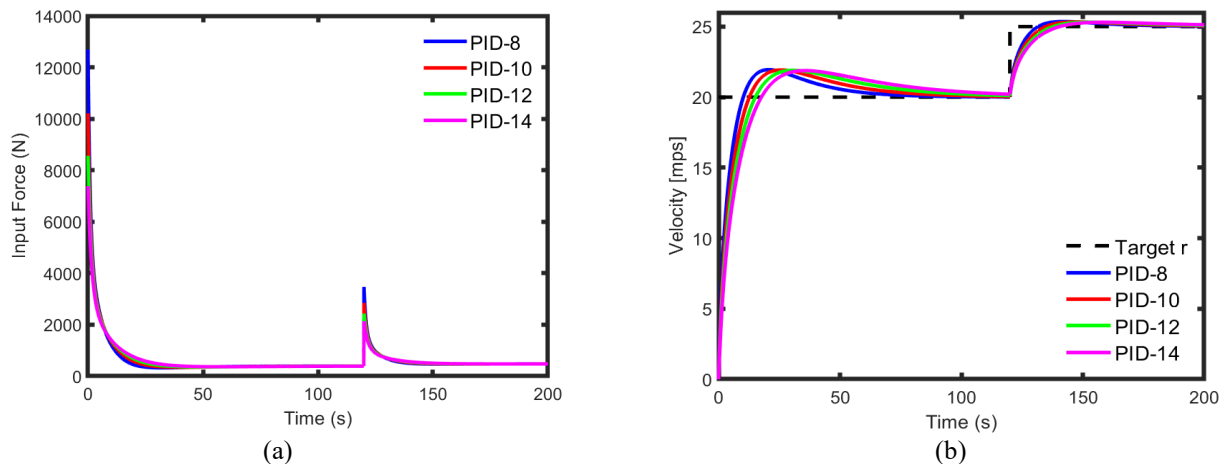


Figure 3. Closed-loop input and output of PID controller with varying tuning values.

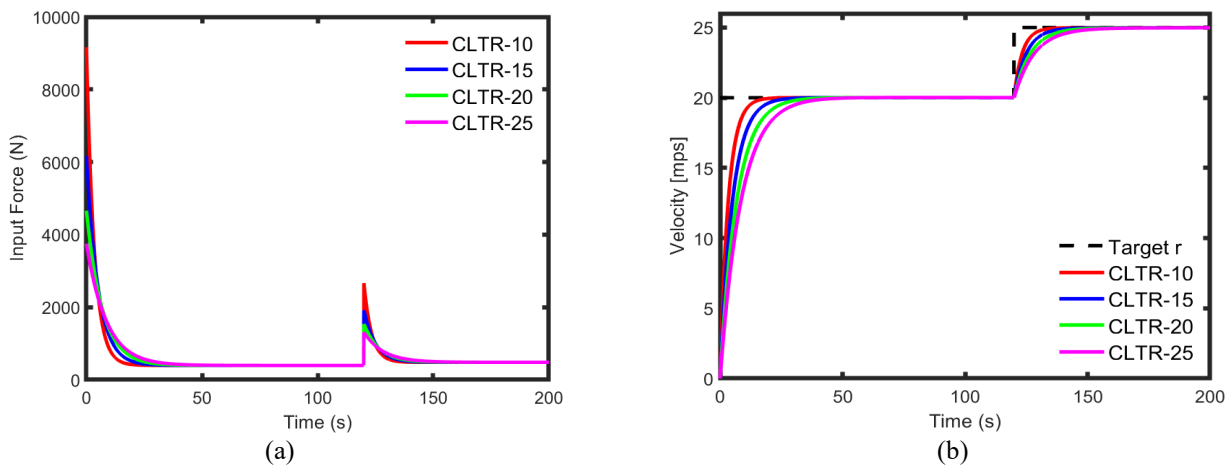


Figure 4. Closed-loop input and output of PFC controller with varying tuning CLTR.

Conversely, PFC is tuned by selecting the desired CLTR corresponding to the time required to reach 95% of the steady-state value. In this case, the number of coincidence horizon is fixed to 1, as discussed in Remark 2. Figure 4 shows the closed-loop behaviour of PFC with a varying selection of CLTR. From the observation, it is noted that the actual response is a close representation of the demanded CLTR. The response also seems to converge to the target value monotonically with less overshoot and less aggressive input demand than the PID controller. In an actual application, this response will provide less fuel consumption and a more comfortable driving experience.

Unconstrained Closed-Loop Response

For a fair comparison, both PID and PFC controllers are tuned to have the same CLTR. The response time of PID is tuned to 14 s, which in return generates three PID gains of $P = 209.5$, $I = 5.294$ and $D = 268.4$. These correspond to 14.8 s of CLTR, which have been set in the PFC algorithm as the tuning parameter. As shown in Figure 5, both controllers' responses intersect at 14.8 s at the speed of 19 m/s (denoting 95% from the desired speed of 20 m/s). A similar finding as

the previous section can be observed where for the unconstrained system, the PID controller requires higher tractive force (7382 N) than PFC (6000 N) to get a similar response. Besides, PFC converges and settles faster and smoother to the desired speed with less overshoot compared to the PID controller.

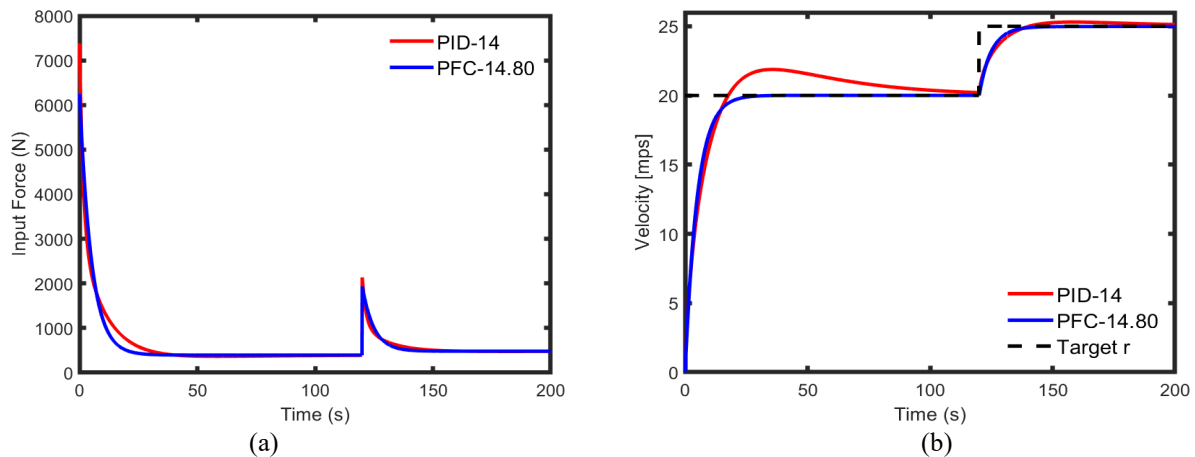


Figure 5. Unconstrained response of PID and PFC controller.

Besides, some quantitative comparisons are presented as shown in Table 3. These parameters are the rise time τ_r , the settling time τ_s , the minimum settling, the maximum settling, the percentage of overshoot M_p %, the peak value (m/s), the peak time τ_p , and the RMSE. These quantitative values are measured in the duration of the first 120s for tracking 20 m/s from rest and will be the controllers' performance indices. As discussed in the earlier finding of Figure 5, it can be observed that the PID controller for the unconstrained closed-loop response requires longer settling times (84.6833 s) as compared to PFC (19.3390 s). These are due to the overshoot percentage produced by the PID controller (8.2902 %), which is comparably higher than PFC (0.0159 %). The PFC controller demonstrates the best-fit response curve to the desired speed of 20 m/s with a lower RMSE of (2.9200) compared to the PID controller's RMSE of (3.2110).

Table 3. Performance indices for both controllers (Unconstrained Case).

Performance Criteria	PID	PFC
Rise time, τ_r	12.5358	10.9190
Settling time, τ_s	84.6833	19.3390
Settling Min., (m/s)	18.2266	18.0234
Settling Max., (m/s)	21.8780	20.0069
Overshoot, M_p %	8.2902	0.0159
Peak, (m/s)	21.8780	20.0069
Peak time, τ_p	35.6000	54.0000
RMSE	3.2110	2.9200

Constrained Closed-Loop Response

For this case, only one input constraint will be considered where the maximum tractive force is limited to 2500 N for both PID and PFC. Figure 6 shows that both PFC and PID responses become slower due to the implemented input constraints from 0 to 100 s. However, PFC provides a better response where it takes less time to converge and settle with minimum overshoot compared to the PID controller. In extreme cases, PID controller may provide oversaturation or integral wind up since no information regarding the constraints is known a priori which is quite different from predictive controller methodology.

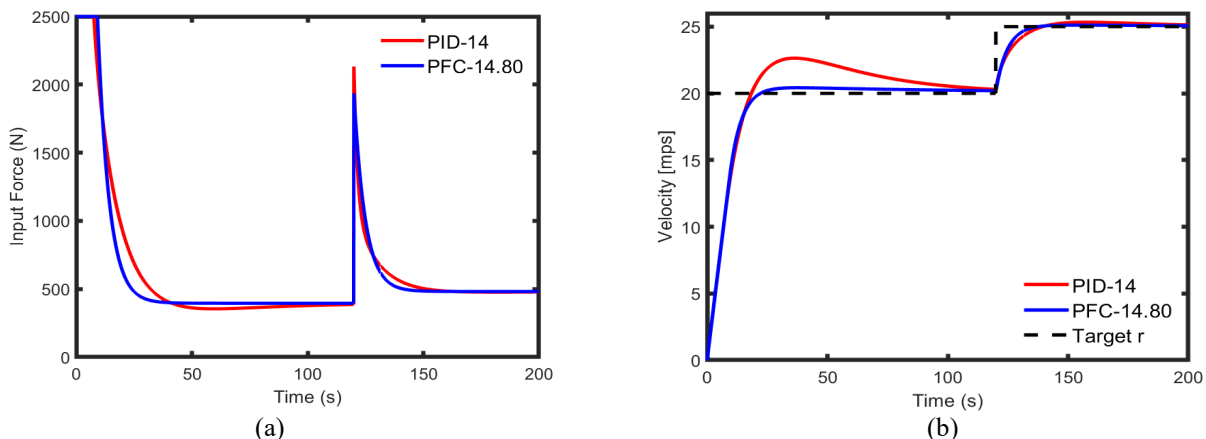


Figure 6. Constrained performance in terms of tractive force for PID and PFC controller.

In addition, Table 4 shows the numerical performance comparison of both PFC and PID controllers. In the first 120 seconds for tracking 20 m/s from rest, the PID controller requires longer settling times (92.0214 s) than the PFC (20.4469 s) for the constrained closed-loop response. These are due to the overshoot percentage produced by the PID controller (11.5468 %), which is comparably higher than PFC (1.1181 %). Although both controller responses become slower due to the implemented input constraints of 2500 N the PFC controller managed to demonstrate the best-fit response curve to the desired speed of 20 m/s with a lower RMSE of (3.9525) compared to the PID controller's RMSE of (4.2166).

Table 4. Performance indices for both controllers (Constrained Case).

Performance Criteria	PID	PFC
Rise time, τ_r	13.6247	13.2790
Settling time, τ_s	92.0214	20.4469
Settling Min., (m/s)	18.2657	18.2006
Settling Max., (m/s)	22.6360	20.4190
Overshoot, M_p %	11.5468	1.1181
Peak, (m/s)	22.6360	20.4190
Peak time, τ_p	36.4000	37.8000
RMSE	4.2166	3.9525

Closed-Loop Response in the Presence of Disturbances.

Figure 7 shows the performance comparison where both controllers manage to handle all the disturbances. However, when there is an inclination disturbance, PID speed drop lower than PFC yet converge faster to the desired speed. This response, in return, requires large over actuation as seen in the input graph at 400s which may lead to more fuel consumption.

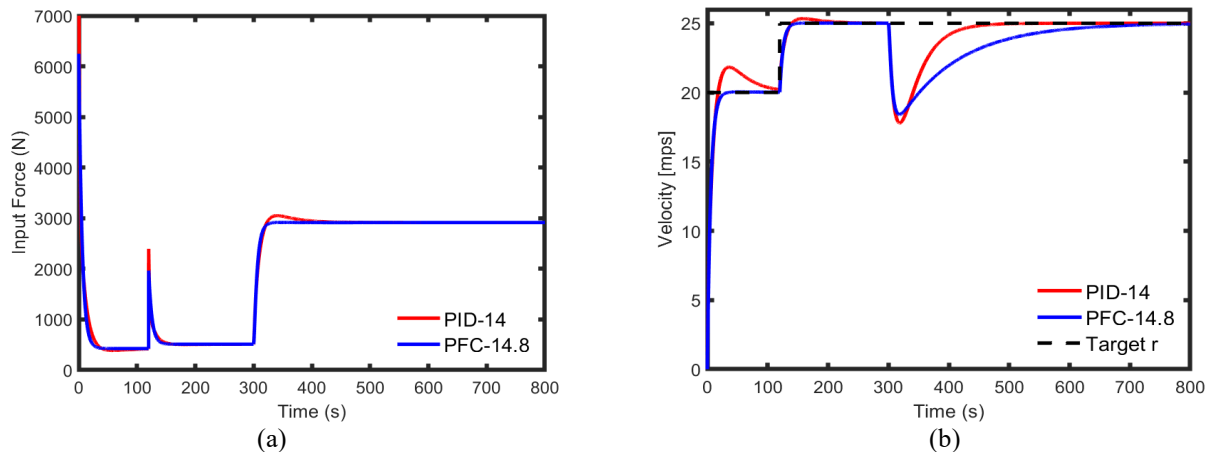


Figure 7. Constrained performance in the presence of disturbance.

CONCLUSION

In summary, this work provides a closed-loop comparison between PID and PFC that are simulated using a simplified nonlinear vehicle longitudinal dynamics model. The main highlight that can be pointed out is that the tuning scheme of PFC is more intuitive and significant in nature compared to the PID. Besides, when both controllers are tuned to achieve a similar closed-loop time response, PFC converges and settles to the desired target faster with less overshoot than the PID controller. Similar observation can be seen when input constraint is implemented. As for the disturbance rejection capability, since PFC considered the constraint information a priori, the speed drops less than PID and converges slower to the target setpoint, which uses less fuel consumption. Future work will investigate the capability of a nonlinear PFC controller for the cruise control system to further improve the closed-loop performance in a different speed driving range.

ACKNOWLEDGEMENT

The authors would like to acknowledge International Islamic University Malaysia Research Management Center Grant 2020 (RMCG20-010-0010) for funding this work. The first author would like to acknowledge Majlis Amanah Rakyat (MARA) for his tuition fee waiver.

REFERENCES

- [1] Y. He *et al.*, "Adaptive cruise control strategies implemented on experimental vehicles: A review," *IFAC-PapersOnLine*, vol. 52, no. 5, pp. 21–27, 2019, doi: 10.1016/j.ifacol.2019.09.004.
- [2] S. E. Shladover, C. Nowakowski, X.Y. Lu, and R. Ferlis, "Cooperative adaptive cruise control: Definitions and operating concepts," *Transp. Res. Rec.*, vol. 2489, no. 1, pp. 145-152, 2015, doi: 10.3141/2489-17.

- [3] R. Pradhan, S.K. Majhi, J.K. Pradhan, and B.B. Pati, "Performance evaluation of PID controller for an automobile cruise control system using ant lion optimizer," *Eng. J.*, vol. 21, no. 5, pp. 347-361, 2017, doi: 10.4186/ej.2017.21.5.347.
- [4] C. Massera Filho, M.H. Terra, and D.F. Wolf, "Safe optimization of highway traffic with robust model predictive control-based cooperative adaptive cruise control," *IEEE Trans. Intell. Transp. Syst.*, vol. 18, no. 11, pp. 3193-3203, 2017, doi: 10.1109/TITS.2017.2679098.
- [5] A. Rahnama, M. Xia, S. Wang, and P.J. Antsaklis, "Passivation and performance optimization using an extremum seeking co-simulation framework with application to adaptive cruise control systems," In *2016 American Control Conference (ACC) IEEE*, pp. 6109-6114, 2016, doi: 10.1109/ACC.2016.7526629.
- [6] S.E. Li *et al.*, "Performance enhanced predictive control for adaptive cruise control system considering road elevation information," *IEEE Trans. Intell. Veh.*, vol. 2(3), pp. 150-160, 2017, doi: 10.1109/TIV.2017.2736246.
- [7] S.E. Shladover, C. Nowakowski, X.Y. Lu, and R. Ferlis, "Cooperative adaptive cruise control: Definitions and operating concepts," *Transp. Res. Rec.*, 2015, vol. 2489(1), pp. 145-152., doi: 10.3141/2489-17.
- [8] S. Park, H. Rakha, K. Ahn, and K. Moran, "Predictive eco-cruise control: Algorithm and potential benefits," In 2011 IEEE Forum on Integrated and Sustainable Transportation Systems, 2011, pp. 394-399, doi: 10.1109/FISTS.2011.5973639.
- [9] M.K. Rout, D. Sain, S.K. Swain, and S.K. Mishra, "PID controller design for cruise control system using genetic algorithm," In 2016 International Conference on Electrical, Electronics, and Optimization Techniques (ICEEOT), 2016, pp. 4170-4174, doi: 10.1109/ICEEOT.2016.7755502.
- [10] R. Pradhan, S.K. Majhi, J.K. Pradhan, and B.B. Pati, "Performance evaluation of PID controller for an automobile cruise control system using ant lion optimizer," *Eng. J.*, vol. 21, no. 5, pp. 347-361, 2017, doi: 10.4186/ej.2017.21.5.347.
- [11] R. Pradhan, S.K. Majhi, J.K. Pradhan, and B.B. Pati, "Antlion optimizer tuned PID controller based on Bode ideal transfer function for automobile cruise control system," *J. Ind. Inf. Integr.*, vol. 9, pp. 45-52, 2018, doi: 10.1016/j.jii.2018.01.002.
- [12] M.I. Miftakhudin, A. Subiantoro, and F. Yusivar, "Adaptive cruise control by considering control decision as multistage MPC constraints," In 2019 IEEE Conference on Energy Conversion (CENCON), 2019, pp. 171-176, doi: 10.1109/CENCON47160.2019.8974766.
- [13] J.A. Rossiter, *A first course in predictive control*. CRC press, 2018.
- [14] S.J. Qin, and T.A. Badgwell, "A survey of industrial model predictive control technology," *Control Eng. Pract.*, vol. 11, no. 7, pp. 733-764, 2003, doi: 10.1016/S0967-0661(02)00186-7.
- [15] S.E. Li, Z. Jia, K. Li, and B. Cheng, "Fast online computation of a model predictive controller and its application to fuel economy-oriented adaptive cruise control," *IEEE Trans Intell. Transp. Syst.*, vol. 16, no. 3, pp. 1199-1209, 2014, doi: 10.1109/TITS.2014.2354052.
- [16] R. Haber, J.A. Rossiter, and K. Zabet, "An alternative for PID control: predictive functional control-a tutorial," In 2016 American Control Conference (ACC), 2016, pp. 6935-6940, doi: 10.1109/ACC.2016.7526765.
- [17] J. Richalet and D. Donovan, "Elementary predictive functional control: A tutorial," In International Symposium on Advanced Control of Industrial Processes (ADCONIP), 2011, pp. 306-313.
- [18] M. Abdullah, and J.A. Rossiter, "Alternative method for predictive functional control to handle an integrating process," In 2018 UKACC 12th International Conference on Control (CONTROL), 2018, pp. 26-31, doi: 10.1109/CONTROL.2018.8516787.
- [19] R. Zhang, A. Xue, and F. Gao, "Further ideas on MPC and PFC using relaxed constrained optimization," in *Model Predictive Control*, , Singapore: Springer, 2019, pp. 127-137.,
- [20] U. Kiencke, and L. Nielsen, "Automotive control systems: for engine, driveline, and vehicle", *Meas. Sci. Technology*. vol. 11, no. 12, pp. 1828, 2000.
- [21] R. Rajamani, *Vehicle dynamics and control*, 2nd ed. New York, NY: Springer, 2011.
- [22] Erwin, "Genting Highland-Batang Kali road." [Online] Available: <https://www.climbbybike.com/climb/GentingHighland/10006> [Accessed: June 1st, 2021.]
- [23] J.A. Rossiter, and R. Haber, "The effect of coincidence horizon on predictive functional control," *Processes*, vol. 3, no. 1, pp. 25-45, 2015, doi: 10.3390/pr3010025.
- [24] M. Abdullah, and J.A. Rossiter, "Using Laguerre functions to improve the tuning and performance of predictive functional control," *Int. J. Control*, vol. 94, no. 1, pp. 202-214, 2021, doi: 10.1080/00207179.2019.1589650.
- [25] J.A. Rossiter, and M. Abdullah, "Improving the use of feedforward in predictive functional control to improve the impact of tuning," *Int. J. Control*, vol. 1-12, 2020, doi: 10.1080/00207179.2020.1843075.
- [26] N. Abe, and K. Yamanaka, "Smith predictor control and internal model control-a tutorial," In SICE 2003 Annual Conference 2003, pp. 1383-1387.
- [27] M. Abdullah, and J. A. Rossiter, "Input shaping predictive functional control for different types of challenging dynamics processes," *Processes*, vol. 6, no. 8, pp. 118, 2018, doi: 10.3390/pr6080118.
- [28] M. Abdullah, et al. "Development of constrained predictive functional control using Laguerre function based prediction," *IFAC-PapersOnLine*, vol. 50(1), pp. 10705-10710, 2017, doi: 10.1016/j.ifacol.2017.08.2222.
- [29] D. Argirov, "Proton Perdana (second generation)". [Online] Available: https://en.wikipedia.org/wiki/Proton_Perdana [Accessed: May 28th, 2021].